

# Development of a Regenerative CO<sub>2</sub> Air Capture Process for Sustainable Greenhouses

Simone Morgana Gorny, s.m.gorny@tecnico.ulisboa.pt  
Instituto Superior Técnico, Lisboa, Portugal

(Dated: October 2019)

Climate change due to global warming is a major issue in our day and age, and one of the biggest challenges to overcome as a society. Within the scientific community, it is accepted that anthropogenic CO<sub>2</sub> emissions are a main contributor, and therefore need to be reduced. CO<sub>2</sub> capturing technologies have the advantage of not only allowing the reduction of emissions, but also of removing CO<sub>2</sub> from ambient air. Adsorption of CO<sub>2</sub> on solid amine sorbents is one of the leading methods of capturing CO<sub>2</sub>. This work takes the first steps towards designing an installation that captures CO<sub>2</sub> from ambient air using Lewatit® VP OC 1065 (a solid amine sorbent) to produce a continuous stream of 1% v/v CO<sub>2</sub> enriched air, to be installed in a greenhouse, where the product stream is used to enrich the air around the crops, to increase their growth. Preliminary cost calculations showed that a fluidized bed is the most economic choice for an installation of this scale. Experimental conditions of bed heights, superficial velocity and inlet concentration of CO<sub>2</sub> were tested to determine the most favourable operation parameters in a fluidized bed. In the final design, composed of an adsorption and a desorption columns with circulating sorbent,  $1 \times 10^3$  m<sup>3</sup>/h (20°C, 1 atm) of ambient air are divided between 10 adsorption fluidized beds, while the sorbent circulates from the top stage to the bottom one. Each stage has a 40 cm diameter and 10 cm height. The sorbent, loaded with CO<sub>2</sub>, leaves the bottom stage and flows into the desorber, a multistage fluidized bed with only one air stream as purge, working at 70°C, where the CO<sub>2</sub> is released from the sorbent. This results in a product stream of CO<sub>2</sub> enriched air, with a concentration between 0.5 and 1%. The lean sorbent is recycled back into the top stage of the adsorber. Operational costs were estimated at 180 €/ton<sub>CO<sub>2</sub></sub>.

**Keywords:** CO<sub>2</sub>, air capture, adsorption, amine sorbent, sustainable greenhouses

**Acknowledgement:** This document was written and made publicly available as an institutional academic requirement and as a part of the evaluation of the MSc thesis in Biological Engineering of the author at Instituto Superior Técnico. The work described herein was performed at the Sustainable Process Technology (SPT) Group of the University of Twente (Enschede, The Netherlands), during the period February-August 2019, under the supervision of Michel Schellevis (MSc, PhD Candidate) and Dr.ir. Wim Brilman (Associate Professor), and within the frame of the Erasmus programme. The thesis was co-supervised at Instituto Superior Técnico by Prof. Helena Pinheiro.

## 1. Introduction

Large carbon dioxide (CO<sub>2</sub>) emissions due to human activities are known to cause the climate changes that are already apparent this day and age, and are only prone to become worse. It is crucial to stabilize the levels of CO<sub>2</sub> in the atmosphere, as the average concentration of CO<sub>2</sub> has already increased from 280 ppm during the pre-industrial time to over 400 ppm currently<sup>1</sup>. Based on the prediction of IPCC, by year 2100, the atmosphere may contain up to 570 ppm of CO<sub>2</sub>, causing a rise of mean global temperature of around 1.9°C and an increase in average sea level of 3.8 m.<sup>2</sup>

Due to these dire prospects, strategies to reduce the amount of CO<sub>2</sub> released into the atmosphere are essential, in order to stabilize its level. These begin with reducing or cutting out the use of fossil fuels<sup>3</sup>. However, the switch to carbon free and renewable energy sources poses many socio-economic and political obstacles, due to costs and low environmental mindset of the general population and many political leaders. Therefore, the development of Carbon Capture and Storage (CCS) technologies is important. The most developed of these technologies uses the reversible reaction of CO<sub>2</sub> with amines to remove the CO<sub>2</sub> from a gas stream, and compress it into empty natural gas reserves. The advantage of CO<sub>2</sub> capture is that it

can be retrofitted to existing facilities, without significant changes to the infrastructure of the energy plant<sup>4</sup> or to the current process, or to the consumers, which is beneficial considering the societal inertia in dealing with climate change<sup>3</sup>.

CO<sub>2</sub> capture is not limited to flue gases in power plants, as it can be applied to Direct Air Capture (DAC) as well. CO<sub>2</sub> capture from ambient air is one of the few options to mitigate emissions from distributed sources, which account for one-third to half of the total anthropogenic CO<sub>2</sub> emissions.<sup>3</sup>

Even though CCS prevents the CO<sub>2</sub> release into the atmosphere and is a good option for mitigation of global warming, the storage of CO<sub>2</sub> is not the only option. As there is a market for CO<sub>2</sub>, the carbon capture technology can be joined to the CO<sub>2</sub> needs in several industries that have use for it, for instance, the captured CO<sub>2</sub> can be used in the carbonated beverages industry, for urea production, fertilizer production, foam blowing and dry ice production<sup>2</sup>. If CO<sub>2</sub> becomes the carbon source for the industry, as some believe, this technology will be its basis. Another use for it, and which is already done in some specific cases in the Netherlands, is in industrial greenhouses, where CO<sub>2</sub> is supplied for a higher concentration in the air, which increases the productivity of the cultures, all year round.

### Scope of the Project

A lot of the food supply nowadays is cultivated in greenhouses, seeing as there are many advantages in growing crops and other plants in closed controlled setups as opposed to directly exposed to the atmosphere. Greenhouses provide protection from atmospheric conditions and climate control. A good control of the climate of the greenhouse leads to higher yields and better quality of the crops, and even extend the growing season to all year round. As plants assimilate CO<sub>2</sub>, its concentration in the greenhouse environment is a relevant parameter to control. Crop yield and quality increases under enrichments of CO<sub>2</sub> to ambient air concentrations of 700-900 ppm.<sup>5</sup>

The CO<sub>2</sub> can be supplied through various ways but, in Northern Europe, it is common to supply industrial CO<sub>2</sub> that comes in liquid form. It is heated and given in gas form through a pipe along the roots or stems of the plants. The DAC technology can be applied here. The suggested solution is having the air inside the greenhouse circulate through a carbon capture column before being released either into the atmosphere or back into the greenhouse. The CO<sub>2</sub> that is adsorbed in the column onto the sorbent is then desorbed by increase of temperature and can be provided to the crops in either pure form or as CO<sub>2</sub>-enriched air. This way, less industrial CO<sub>2</sub> needs to be supplied, and less of it is wasted. The overall purpose of this thesis is to come to a design of a scalable CO<sub>2</sub> capture installation and process layout that can be implemented in existing greenhouses to minimize their carbon footprint.

## 2. Background & Theory

### 2.1. Carbon Capture with solid sorbents

The CO<sub>2</sub> capture process with amines can be either by absorption by aqueous alkanolamine solutions or adsorption by solid amine sorbents, both at low temperatures. When the temperature increases, the reaction is reversed and the CO<sub>2</sub> is released. Absorption by amine solvents is a developed method for power plants, but energy intensive. Processes based on adsorption of CO<sub>2</sub> by solid sorbents are currently being developed as regeneration of solid sorbents requires much less energy than the solvent systems<sup>6</sup>. This is due to the lower heat capacity of the solid support compared to the aqueous support in an absorption process.<sup>7</sup>

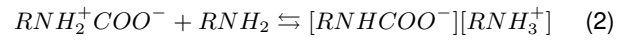
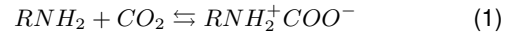
Solid supports for amine sorbents are highly porous materials, with a high internal surface area and functionalized amine groups either immobilized on or grafted into the surface. The aspects of these sorbents that are looked at when choosing an appropriate one are CO<sub>2</sub> capacities, CO<sub>2</sub> uptake rates, necessary heats of absorption and regeneration conditions. In a typical adsorption separation process for CO<sub>2</sub> capture with solid sorbents, the gas to be treated is contacted with a lean sorbent at low temperatures and CO<sub>2</sub> is preferentially adsorbed onto the material. Once the sorbent is saturated, it is then regenerated by promoting the desorption of CO<sub>2</sub>.<sup>8</sup>

This carbon capture technology can be used both for flue gases and natural gas, and for ambient air. However, DAC is less favourable than CO<sub>2</sub> capture

from flue gases due to the much lower CO<sub>2</sub> concentration in ambient air. Nonetheless, this aspect does not present a limitation on the economics of the DAC process<sup>9</sup>. The main challenge is the massive amount of air to be treated per mass of CO<sub>2</sub> captured<sup>10</sup>. Therefore, air capture methods for DAC cannot be energy intensive.<sup>3</sup>

### 2.2. Adsorption

Lewatit® VP OC 1065 was selected by Veneman<sup>11</sup> as a stable amine sorbent with a good CO<sub>2</sub> capturing capacity, and therefore is used in this research. It is a macroporous, divinylbenzene crosslinked polymer in spherical bead form with primary amine groups. The primary amine functional groups are responsible for the selective adsorption of CO<sub>2</sub>, according to the following pathway.



The extent of the reaction is bound by equilibrium, and the amount of a compound that a sorbent can adsorb at a certain temperature is usually determined by isotherms. Previous work<sup>11,12</sup> showed that the Toth isotherm model is the best fit for the experimental CO<sub>2</sub> adsorption data, and is described by the following equations.

$$q^* = \frac{n_s b P_{ads}}{(1 + (b P_{ads})^t)^{1/t}} \quad (3a)$$

$$b = b_0 \exp\left(\frac{\Delta H_r}{RT_0} \left(\frac{T_0}{T} - 1\right)\right) \quad (3b)$$

$$t = t_0 + \alpha \left(1 - \frac{T_0}{T}\right) \quad (3c)$$

$$n_s = n_{s0} \exp\left(\chi \left(1 - \frac{T}{T_0}\right)\right) \quad (3d)$$

Where  $q^*$  is the loading of the sorbent in mol<sub>CO<sub>2</sub></sub>/kg<sub>sorb</sub>,  $b$  is the equilibrium constant,  $t$  describes the heterogeneity of the adsorbent,  $\Delta H_r$  is the isosteric heat of adsorption,  $R$  is the gas constant and  $T_0$  is the reference temperature. The parameters  $\alpha$  and  $\chi$  determine the dependence of temperature relative to the reference temperature  $T_0$  for  $t$  and  $n_s$ , respectively. When considering chemisorption, the number of available sites is determined by the number of molecules on the adsorbent, which is independent of temperature. Therefore,  $\chi$  is always equal to zero for chemisorption.<sup>13</sup>  $P_{ads}$  and  $T$  are the operation conditions of partial pressure of CO<sub>2</sub> and temperature, respectively.

The parameters, determined by M. Bos *et.al.*, used in this equilibrium model are present in Table I<sup>12</sup>. Figure 1 shows adsorption capacities determined by M. Bos *et.al.* using the equilibrium model, fitted to experimental results.

### 2.3. Desorption

Desorption can be done in a few different ways: decreasing the pressure, Pressure Swing Adsorption (PSA); increasing the temperature, Temperature Swing Adsorption (TSA); or adding a purge gas, Concentration Swing Adsorption (CSA).

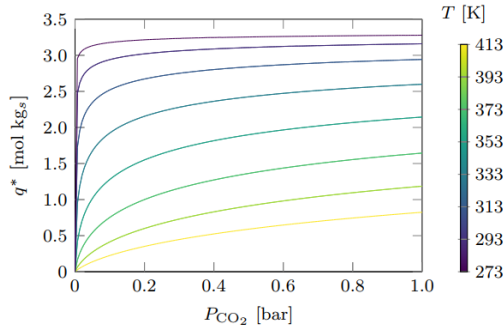


**FIG. 1:** CO<sub>2</sub> adsorption isotherms for Lewatit® VP OC 1065 from 273 K to 413 K with 20 K intervals. The lines represent capacities calculated using the equilibrium model.<sup>12</sup>

**TABLE I:** Toth isotherm parameters of the adsorption of CO<sub>2</sub> on Lewatit® VP OC 1065 using 353 K as reference temperature, as determined by M. Bos, *et. al.*<sup>12</sup>

Parameter	Value
$t_0$	0.37
$b_0$ (bar <sup>-1</sup> )	93.0
$n_{s0}$ (mol/kg)	3.40
$\chi$	0
$\alpha$	0.33
$\Delta H$ (J/mol)	$95.3 \times 10^3$

These processes can be illustrated from the adsorption isotherm, whose principles of PSA and TSA are represented in Figure 2, where the principle of CSA is similar to that of PSA.<sup>13,14</sup>

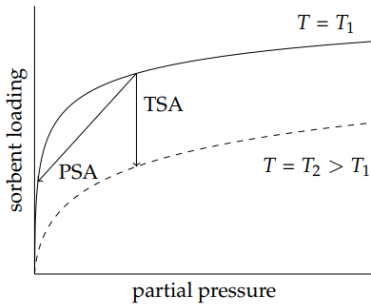


**FIG. 2:** Illustration of temperature swing adsorption (TSA) and pressure swing adsorption (PSA)

Often, the desorption process is performed under a combination of these principles. The gas used as purge is commonly either nitrogen, air, or steam. When using nitrogen or air, the product CO<sub>2</sub> is not pure, but rather a CO<sub>2</sub>-enriched stream. If air is used as purge, the sorbent cannot be completely regenerated, because air contains CO<sub>2</sub> in an average concentration of 400 ppm. When using steam, as it is easily condensable, a simple cooling treatment of the product stream can produce pure CO<sub>2</sub>.

The working capacity of the sorbent depends on the adsorption and desorption conditions, which determine the equilibrium capacity of each process. The difference between them is the working capacity (equation 4), which is an important parameter in process design.

$$\Delta q_w = q_{\text{adsorption}}^*(p, T) - q_{\text{desorption}}^*(p, T) \quad (4)$$

## 2.4. Sorbent degradation

The sorbent's stability is a very important factor in the viability of an adsorption process. If it is unstable and has to be replaced often, it can quickly become economically intensive, and can be restrictive about the conditions in which the reaction is processed.

Qian Yu, *et. al.*, showed that there was no loss of capacity of the sorbent when exposed to temperatures up to 150°C in nitrogen. Compared to other sorbents, namely the ones impregnated with amines instead of bound to, the Lewatit particles show great thermal stability<sup>11</sup>.

The stability in CO<sub>2</sub> was also studied. If the partial pressure of CO<sub>2</sub> approaches 1 bar, the maximum temperature should not be higher than 120°C as to avoid the formation of urea<sup>10</sup>. In the presence of oxygen, the degradation is more significant already at temperatures above 70°C<sup>10</sup>.

Qian Yu, *et. al.*, also showed that there is no difference in stability between continuous and cyclic treatment, and therefore the cyclic adsorption-desorption has no effect on sorbent degradation<sup>10</sup>.

## 3. Reactor design

### 3.1. Fluidized Bed Reactor

The purpose of the installation is one that can provide 1 kg/h of CO<sub>2</sub> continuously, in the form of 1% v/v CO<sub>2</sub>-enriched air. Preliminary calculations and analysis of the available options showed that a fluidized bed reactor is a good choice for an installation of this scale.

In a fluidized bed reactor, the solid sorbent is fluidized by the gas stream. The linear velocity of the gas stream is kept above the minimum fluidization velocity ( $u_{mf}$ ), otherwise the bed will behave as a fixed bed. Minimum fluidization occurs when the pressure drop ( $\Delta P$ ) over the bed equals the weight of the particles, as described by equation 5, and is usually determined experimentally.

$$\Delta P = (\rho_p - \rho_g)(1 - \varepsilon_{mf})g \cdot L_{mf} \quad (5)$$

Where  $\rho_p$  is the particle density,  $\rho_g$  is the gas density,  $\varepsilon_{mf}$  is the bed porosity at minimum fluidization,  $g$  is the gravity force and  $L_{mf}$  is the bed length (height) at minimum fluidization.

The higher the superficial velocity of the gas stream, the more the bed expands. When the superficial velocity equals the terminal velocity of the particles, these escape the reactor.<sup>15</sup>

At superficial velocities above minimum fluidization velocity, the pressure drop is close to constant<sup>16</sup>. Therefore, the pressure drop depends only on the bed height at minimum fluidization, which is determined by equation 6,  $V_{\text{sorbent}}$  being the volume of sorbent in the bed, and  $A$  the surface area of the bed. Driessen, *et. al.*, determined the minimum fluidization velocity and bed porosity at minimum fluidization of Lewatit VP OC 1065 experimentally, as 0.091 m/s and 0.51, respectively<sup>17</sup>.

$$L_{mf} = \frac{V_{\text{sorbent}}}{(1 - \varepsilon_{mf})A} \quad (6)$$

### 3.2. Design basis

For low costs of CO<sub>2</sub> adsorption from the air in the greenhouse, the performance of the reactor is important. This depends on feed conditions, reactor dimensions and operating conditions. One relevant performance indicator is the adsorption rate, meaning, the time it takes to achieve a certain loading of CO<sub>2</sub> on the sorbent. The adsorption rate can be determined experimentally through the breakthrough curve. The adsorption time can be compared to the stoichiometric adsorption time, which is the theoretical time it would take to reach equilibrium loading if the CO<sub>2</sub> adsorption was instant and complete. The stoichiometric time ( $t_{stoich}$ ) at 100% loading can be calculated with the ratio between the CO<sub>2</sub> loading and the amount of CO<sub>2</sub> in the feed. This is described in equation 7, where  $m_s$  is the mass of sorbent in the bed,  $\varphi_v$  is the feed flow rate and  $C_{CO_2}$  is the concentration of CO<sub>2</sub> in the feed.

$$t_{stoich} = \frac{CO_2 \text{ capacity (mol)}}{CO_2 \text{ feed (mol/s)}} = \frac{m_s q_e}{\varphi_v C_{CO_2}} \quad (7)$$

In order to evaluate the energy intensity of the process, the required energy demands can be calculated. First, the sensible heat to be transferred to the sorbent,  $Q_{sensible \text{ sorbent}}$  is calculated using equation 8, using the temperature difference between the adsorption and the desorption, where  $C_{p,s}$  is the heat capacity of the sorbent and  $T$  is the temperature.

$$Q_{sensible \text{ sorbent}} = m_s \cdot C_{p,s} (T_{desorption} - T_{adsorption}) \quad (8)$$

As the desorption reaction of the CO<sub>2</sub> from the sorbent is endothermic, energy supply is necessary to release the CO<sub>2</sub> from the amine. The amount of energy required, per kilogram of CO<sub>2</sub>, is calculated from the reaction heat, with equation 9.

$$Q_{reaction \text{ heat}} = \frac{\Delta H_r}{MW_{CO_2}} \quad (9)$$

As the sensible heat taken up by the CO<sub>2</sub> is determined by equation 10, where  $C_{p,CO_2}$  is the heat capacity of CO<sub>2</sub>.

$$Q_{sensible \text{ CO}_2} = C_{p,CO_2} (T_{desorption} - T_{adsorption}) \quad (10)$$

To reduce the pressure inside the reactor and overcome the pressure drop from the flow rate through the sorbent particles, energy is required to compress the air. Adiabatic compression is assumed, and calculated by equation 11.

$$Q_{air \text{ compression}} = \frac{1}{\eta} \cdot \frac{k}{k-1} \cdot \dot{\phi}_{mole, CO_2} \left( 1 + \frac{1}{ratio(CO_2/purge)} \right) \cdot RT \left[ \left( \frac{p_2}{p_1} \right)^{k-1/k} - 1 \right] \cdot t \quad (11)$$

The efficiency of the compression,  $\eta$ , is assumed to be 0.75, and the ratio of  $C_p/C_v$ ,  $k$ , is 1.3 for air<sup>18</sup>.  $\dot{\phi}_{mole, CO_2}$  is the molar flow of CO<sub>2</sub>,  $ratio(CO_2/purge)$  is the molar ratio of CO<sub>2</sub> in the total gas flow,  $R$  is the gas constant and  $T$  is the temperature at which the operation is performed. In the case of gas compression to overcome pressure drop,  $p_2$  is  $\Delta P + p_{atm}$  and  $p_1 = p_{atm}$  is assumed to be 1 bar and  $t$  is either the time of the adsorption or the time of the desorption.

In fluidized beds, increasing superficial velocities above minimum fluidization, increases the bubble phase and the flow becomes turbulent. As a result, channelling occurs and the contact between air and solid decreases, decreasing the efficiency. The channelling effect also increases due to bubble formation when the bed is wider and higher, as the size of the bubbles increases between the moment they are formed at the distributor and the top of the bed. This can be an issue when scaling up. However, if the height remains low, the channelling effect is likely to be low.<sup>19</sup>

Lower superficial velocities has also proven to result in lower outlet gas concentrations (when working in continuous mode) and higher tray efficiencies (when working in multistage setup)<sup>19</sup>. With lower superficial velocities, the gas contact time is longer, allowing more time for the CO<sub>2</sub> to be adsorbed onto the sorbent and reaching equilibrium loading. However, with higher superficial velocities the amount of CO<sub>2</sub> inserted in the system is higher, thus the sorbent gets into contact with higher quantities of CO<sub>2</sub> over time. Therefore, a trade-off must be found, a high enough superficial velocity that maximizes the amount of CO<sub>2</sub> inlet, and maximizes the residence time and contact with the sorbent, without increasing the gas bypass. This trade-off of superficial velocities must also be combined with the trade-off of bed heights, as a shallow bed decreases bubble size and therefore channelling, but a bigger bed height increases the contact time of the phases.

To capture 1 kg CO<sub>2</sub>/h, a flow rate between 1500 and 2700 m<sup>3</sup>/h (depending on contact efficiencies and concentrations of CO<sub>2</sub> in the air) is needed. To flow through shallow beds at a low superficial velocities, a big surface area is necessary. In a single vessel, the diameter of the adsorption bed would have to be from 1 to 2.5 m to keep the mentioned flow rates at a low superficial velocity low. Meanwhile, the desorption requires a flow rate of 55 m<sup>3</sup>/h to produce enriched air of 1% CO<sub>2</sub>. For low superficial velocities, the required bed diameter is 40 cm. This is a more reasonable dimension, and as in practical terms it is easier if the adsorber and the desorber have the same dimensions, the adsorber can be divided in several stages of 40 cm diameter each, and the inlet gas stream is divided through the different stages. These different stages can be stacked up on top of each other, much like a multistage fluidized bed, where the lean sorbent enters at the top stage and flows down, from stage to stage, until it leaves the bottom stage loaded with CO<sub>2</sub>. Each stage has an air inlet and outlet, therefore, the sorbent in each stage is contacted with new air. The design of an adsorption stage is shown in Figure 3.

From the bottom stage of the adsorber, the sorbent will fall into the desorber, that, for increased efficiency, has several stages in the traditional disposition: air inlet in the bottom, air outlet at the top, flowing through all the stages. The desorption, can done with air as purge, because it is available and it requires no additional investment, as opposed to pure nitrogen or steam. This means, however, that the desorption will be performed in the presence of oxygen, thus cannot go above 70°C, otherwise the degradation of the sor-

bent is significant<sup>10</sup>.

The heating of the stages in the desorber can be done by heat tracing on the outside of each stage, but, as the diameter is considerable also the plates on which the sorbent rests can be heated. By contact with the warm plates, the air will increase in temperature as well and contribute to the heating of the sorbent. The fluidization itself induces the mixing and homogenization of the bed, providing better heat transfer.

The lean sorbent, at 70°C, leaves the bottom of the desorber, its flux controlled by a rotary valve, and into a riser. The riser has a flow of ambient air that transports the sorbent to the top of the adsorber, while it is cooled with cold water on the outside, and by the cool air itself. At the top of the riser a cyclone separates air from the sorbent, and the lean sorbent enters the top stage of the adsorber once more. The sorbent is, however, not entirely lean. As the desorption is performed with air, which contains CO<sub>2</sub>, the sorbent will leave the desorber at the equilibrium loading at these conditions, 0.21 mol/kg, value obtained from the Toth isotherm seen in section 2.

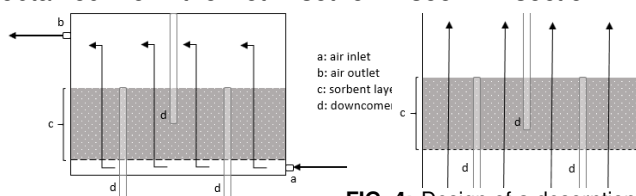


FIG. 3: Design of an adsorption stage

FIG. 4: Design of a desorption stage

The exact dimensions and number of stages, both in the adsorber and the desorber, as well as the superficial velocity and sorbent flux, can not be defined as of yet. To do so, experimental data is necessary, to determine which design parameters and operation conditions can provide the desired output of 1 kg/h of CO<sub>2</sub>, at a relative low cost. This experimental data was obtained using a setup described in the next section.

#### 4. Experimental

For the experimental part of this assignment, a multi-stage fluidized bed (MSFB) set-up was used. The set-up is comprised of an adsorber, a desorber and a riser, which allows sorbent circulation. The set-up can be seen on Figure 5.

The adsorption column is constructed in modules, which can be added or removed in order to increase or decrease the number of stages. There are five stages in total. Each module is 15 cm tall and has a 10 cm internal diameter, and can be stacked on top of each other and held air-tightly together by flanges. One stage is made of two modules, with a perforated plate (triangular pitch of round holes, 0.5 mm hole diameter, 1.5 mm hole pitch) on the bottom one, and two standpipes (13 mm internal diameter) which allow the sorbent to overflow to the next stage. The height of the standpipes above the perforated plate can be adjusted to vary the bed height. At the lowest stage, a metal sintered plate is installed instead of a perforated plate to ensure an even initial distribution of gas. Each stage was fitted with a sample point in the freeboard, connected to a LI-COR LI-840A CO<sub>2</sub> analyzer (calibration range: 0 - 10000 mol ppm CO<sub>2</sub>). Besides this,

K-type thermocouples were installed at each stage 20 mm above the distributor, as well as at the gas inlet to the adsorber. Figure 5 shows the overview of the setup and the internals of the adsorber in more detail.

The desorber is a five stage fluidized bed, with internal diameter 10 cm. In the desorber, the number of stages cannot be changed. Each stage is equipped with heat tracing, in order to heat up the stages to desorption temperature (~110°C). These stages are also defined by perforated plates with standpipes to allow the overflow of sorbent to the following stage. The bottom stage is connected to a rotary valve which regulates the sorbent flux into the riser. The sorbent rises by a flow of nitrogen, while it is cooled by water on the outside.

The gas flow in any part of the set-up is controlled by mass flow controllers (MFCs). The nitrogen flow to the adsorber is controlled by two MFCs: a Brooks Instrument 5851 MFC (0-70 L min<sup>-1</sup>) and a Brooks Instrument 5851E MFC (0-100 L min<sup>-1</sup>). The CO<sub>2</sub> flow is controlled by a Brooks Instrument MFC (0-150 mL min<sup>-1</sup>). These three inlet flows are mixed before entering the adsorber. The riser gas flow is controlled with a Brooks Instrument 5850 MFC (0-11 L min<sup>-1</sup>). The gas flow to the desorber is regulated by a Brooks Instrument 5851S MFC (0-100 L min<sup>-1</sup>). All MFCs were carefully calibrated using appropriate gas flow measuring devices.

In both the adsorber and the desorber, the gas inlet is at the bottom stage, and is contacted with each stage until flowing out at the top. The sorbent flows in at the top of the column and leaves at the bottom. The sorbent is fluidized by the gas flow, with the overflow falling through the standpipes into the stage below. From the bottom stage of the adsorber, the overflow of sorbent goes into the desorber, its flux being regulated by a rotary valve. In the desorber, the sorbent is stripped of its CO<sub>2</sub> content by a nitrogen purge. The resulting flue gas exits the column at the top. At the bottom of the desorber, a rotary valve determines the solid flux to the riser. The riser is a long, thin tube (8.5 mm internal diameter) with a cooling jacket around it that connects the bottom of the desorber with the top of the adsorber. The sorbent is transported by a nitrogen flow to the top of the adsorber at a superficial velocity of ~3.5 m/s, where a cyclone separates the sorbent from the nitrogen flow and the fines. The lean sorbent then enters the top of the adsorber again.

The experiments performed in this report were executed with a single stage adsorber, meaning, the remaining four stages were removed. The breakthrough curves of adsorption were obtained from performing the adsorption in a single stage, without circulation of the sorbent. The regeneration between experiments was done at ~110°C with circulation.

#### 5. Results & discussion

The breakthrough curves measured in the single stage fluidized bed described in section 4 were obtained for three different flow rates/superficial velocities, each with three different inlet concentrations (400, 600 and 800ppm), and each of these breakthrough measurements were done at two different bed heights (5 and



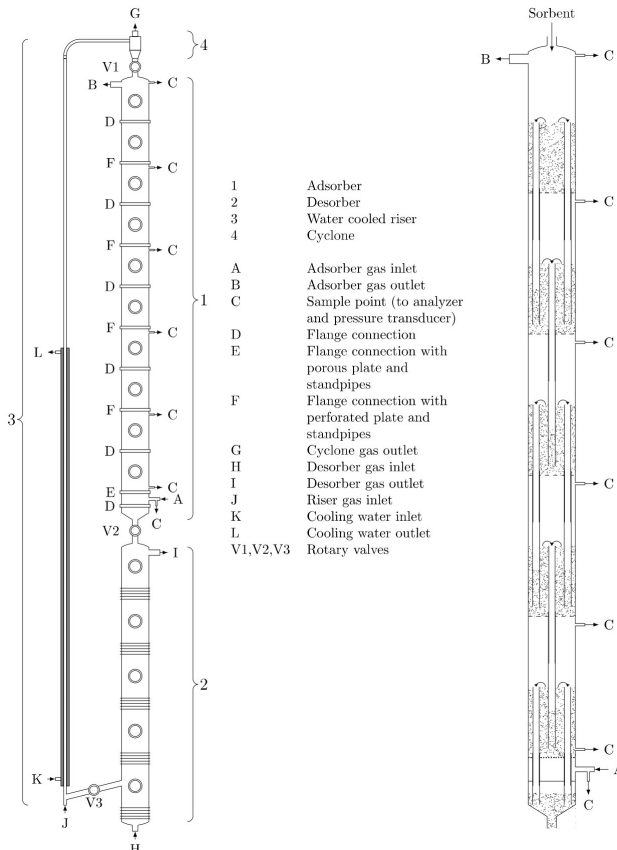


**FIG. 5:** Schematic overview of the multistage fluidized bed setup, and cross-sectional view of the interior of the adsorber<sup>17</sup>

10 cm). The superficial velocities measured were 0.12 m/s, just above minimum fluidization, 0.17 m/s, when there is a visible bubble phase, and 0.23 m/s, with a significant bubble phase.

The output of these breakthrough measurements is the concentration of  $\text{CO}_2$  in the outlet, in ppm. This is then converted into mol of  $\text{CO}_2$  and divided by the mass of sorbent in the bed to obtain the loading of sorbent over time. This is represented in the Figures 6 and 7, each obtained at a constant bed height of 5 and 10 cm, respectively.

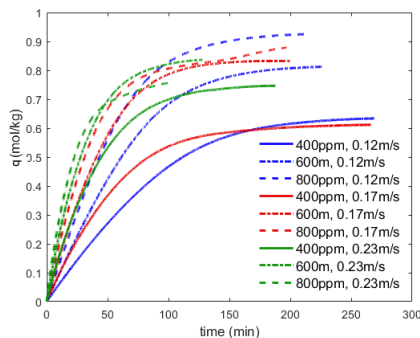


**FIG. 6:** Sorbent loading ( $q$ ) in  $\text{mol}_{\text{CO}_2}/\text{kg}$  in function of adsorption time for breakthrough curves obtained at 400(-), 600(-) and 800(-) ppm inlet concentration and 0.12(blue), 0.17(red) and 0.23(green) m/s of gas phase superficial velocity. Bed height: 5 cm

It can be seen that, no matter the inlet concentration or bed height, the higher the flow rate, the faster the superficial velocity and the quicker the loading of the sorbent is. This is due to, for one, that a bigger

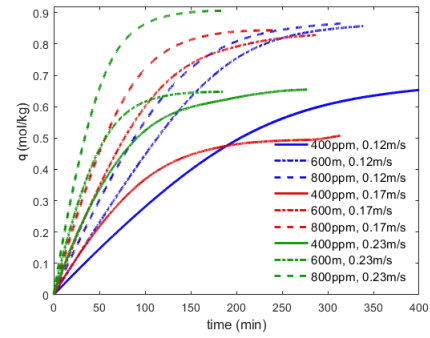


**FIG. 7:** Sorbent loading ( $q$ ) in  $\text{mol}_{\text{CO}_2}/\text{kg}$  in function of adsorption time for breakthrough curves obtained at 400(-), 600(-) and 800(-) ppm inlet concentration and 0.12(blue), 0.17(red) and 0.23(green) m/s of gas phase superficial velocity. Bed height: 10 cm

quantity of  $\text{CO}_2$  is provided to the system over time, therefore, there is more  $\text{CO}_2$  available and coming into contact with the sorbent, which, considering the fast kinetics of the adsorption, will increase the driving force. Secondly, as the flow is more turbulent, there is better mixing of air and sorbent, and better mixing of loaded and lean sorbent within the bed. With a low flow rate and a superficial velocity close to minimum fluidization, the bed is loaded with  $\text{CO}_2$  from the bottom to the top, and only the bottom layer comes into contact with fresh incoming gas. The top of the bed comes into contact with mostly lean gas, meaning, the driving force is very low at this place of the bed. As the superficial velocity increases, so does the bubble phase and with it the turbulence of the bed. This results in a better mixing of the sorbent, with a more homogeneous distribution of adsorbed  $\text{CO}_2$  on the bed.

As for the final loading where the curve reaches the asymptotic value, it cannot be compared between experiments in their absolute value. Because the equilibrium loading of the sorbent is temperature dependent and the set-up does not have temperature regulation on the adsorber, plus they were all performed on different days, the temperature at which the breakthrough curve was obtained differed from one experiment to the other. Therefore, the final loading of the sorbent can only be analyzed in its relative value, as the fraction of the theoretical equilibrium loading, obtained from the Toth isotherm described in chapter 2. However, due to some degradation of the sorbent, the equilibrium loading of the sorbent used was only 70% of the equilibrium loading determined by the isotherm. Therefore, this was taken into account when determining the relative loading of the sorbent over time, which can be seen in Figures 8 and 9.

At a bed height of 5 cm, the lower the superficial velocity the higher percentage of equilibrium loading over stoichiometric time is achieved. This is an indication of the efficiency of the adsorption. The adsorption is more efficient under low superficial velocities, closer to minimum fluidization, as in this regime the bubble phase is very small, and therefore the contact of the solid and gas phase is bigger, with less mass transfer limitations. At a higher flow rate, even though the uptake is faster, as can be seen in Figure 6, it is less efficient because of the bigger bubble phase and

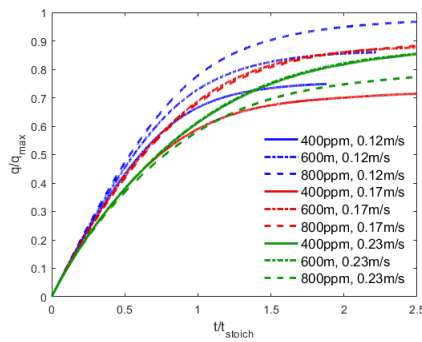


**FIG. 8:** Relative loading of the sorbent in function of relative stoichiometric time for breakthrough curves obtained at 400(-), 600(-) and 800(-) ppm inlet concentration and 0.12(blue), 0.17(red) and 0.23(green) m/s of gas phase superficial velocity.  $q_{max}$  at 70% of the equilibrium capacity obtained from the Toth isotherm. Bed height: 5 cm

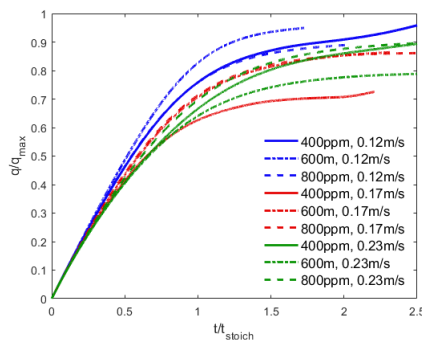


**FIG. 9:** Relative loading of the sorbent in function of relative stoichiometric time for breakthrough curves obtained at 400(-), 600(-) and 800(-) ppm inlet concentration and 0.12(blue), 0.17(red) and 0.23(green) m/s of gas phase superficial velocity.  $q_{max}$  at 70% of the equilibrium capacity obtained from the Toth isotherm. Bed height: 10 cm

therefore bigger mass transfer limitations.

At a bed height of 10 cm, this variation of efficiencies with flow rates is less obvious, at least up to  $t=t_{stoich}$ . This is due to the height of the bed itself, as it increases the contact time between the gas phase and the solid phase and, in result, the effect of the bubble phase is less intense, even though it is still perceivable. Thus, a 10 cm thick bed can be more favourable than a 5 cm thick one.

For the purpose of this assignment, to design a set-up that produces 1 kg/h of  $CO_2$ , it is more relevant that the sorbent adsorbs a large quantity of  $CO_2$  in a short period of time, than that the adsorption is stoichiometrically efficient. So, from this assessment, a higher superficial velocity is more advantageous to achieve a higher  $CO_2$  loading within the adsorption time. So at any given concentration of  $CO_2$  in the inlet, air flows of 0.17 to 0.23 m/s provide a higher sorbent loading within a reasonable adsorption time.

## 6. Design Parameters

### 6.1. Sorbent flux

The amount of  $CO_2$  obtained in the desorption is a function of the sorbent  $CO_2$  loading,  $q$ , and of the sorbent flux. The higher the sorbent flux and the higher its loading the more  $CO_2$  can be obtained. However, as the process is continuous and cyclic, the higher the

sorbent flux in the adsorber, the lower is its residence time, and therefore the lower its  $CO_2$  loading is. This begs the question, is the production higher if the sorbent loading is high, but the sorbent flux low, or vice-versa?

The sorbent flux is inversely proportional to the residence time, for a fixed dimension of the adsorber. The sorbent loading over time can be determined from the breakthrough curves in chapter 5. When testing different values of residence time of the sorbent in the adsorber, both the resulting sorbent loading after leaving the adsorber and the sorbent flux can be calculated. The sorbent loading is determined via the breakthrough curves. With sorbent loading and sorbent flux, the amount of  $CO_2$  obtained after desorption can be determined, in order to answer the pending question. The  $CO_2$  obtained after desorption is calculated assuming the desorption is complete until equilibrium at desorption conditions. Some values of residence time within a reasonable range (10 to 100 minutes) were represented in Figure 10, that were obtained from the breakthrough curve at 600 ppm and 0.23 m/s, to determine what the trend is.

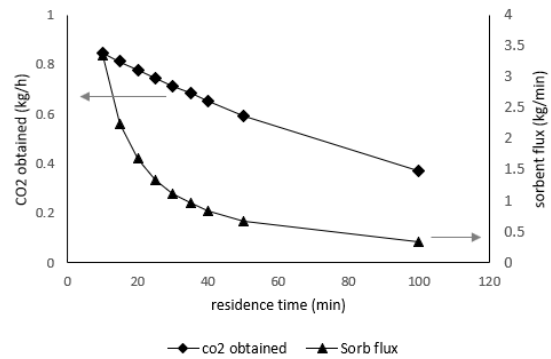


**FIG. 10:** Effect of the residence time of the sorbent in the adsorber on the sorbent flux and amount of  $CO_2$  obtained in the desorber, calculated with sorbent loading values from the breakthrough curve obtained at 600ppm and 0.23 m/s

It is clear that the amount of  $CO_2$  obtained increases when the residence time in the adsorber decreases, even though the loading of the sorbent is lower. This is due to the fast increase of sorbent flux with the lower residence times. Furthermore, no matter how much the residence time increases, the higher sorbent loading will not make up for the low sorbent flux, and the resulting production of  $CO_2$  in the desorber will be lower the longer the residence time. With this, the conclusion is obvious that a lower residence time, thus higher sorbent flux, is advantageous. Nonetheless, high solid flows increase a lot the energy costs and the physical toll on the equipment, mainly the valves and riser.

From a certain sorbent flux (around 60 kg/h) there is no significant increase in the amount of  $CO_2$  obtained, while there is a fast increase in sorbent flux. This is when the increase in sorbent flux and the decrease of sorbent loading are close to canceling each other out. So, a sorbent circulation rate of 60 kg/h was chosen.

With a defined sorbent flux, the dimensions of the riser can be determined. For 60 kg/h, the necessary flow rate of air in the riser with 8 cm of inner diameter is 70  $m^3/h$  (to overcome the gravity force), and the

superficial velocity of the gas is 3.8 m/s.

### 6.2. Adsorption column dimensions

With a defined sorbent flow, the residence time of the sorbent in the adsorber can be defined as well, although it still depends on the number of stages and the height of each stage. A maximum number of stages was set at 10, seeing as this corresponds to an adsorber column of about 2 meters (each stage at 20 cm), and the maximum height of the beds at 10 cm. A thicker bed would increase the bubble phase and decrease the contact efficiency of the bed. Considering that greenhouses have a height of between 3 and 10 meters, it is not wise to design a reactor that does not fit in the smaller greenhouses. With 10 stages and 60 kg/h of sorbent, the four most favourable operating conditions were compared in terms of CO<sub>2</sub> production in the desorber. They can be graphically compared in Figure 11.

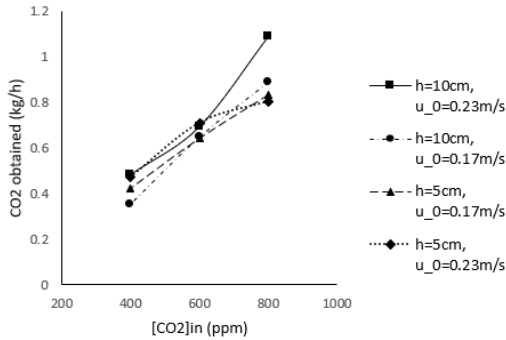


**FIG. 11:** CO<sub>2</sub> production capacity of the desorber in different conditions of bed height and superficial velocities of the inlet air, for 10 stages and sorbent circulation at 60 kg/h in the 400-800ppm range of CO<sub>2</sub> concentration in the inlet air to the adsorber.

For the tested conditions, between 400 and 600 ppm in the treated air in the adsorber, the production of CO<sub>2</sub> in the desorption is quite similar for all. This, however, changes at the higher inlet concentration of 800 ppm, at 10 cm tall beds and 0.23 m/s of superficial velocity, as the production is quite higher than at the other three conditions. Besides, these conditions are the only ones that are capable of providing the goal of 1 kg/h of CO<sub>2</sub>, even if this is only possible when the inlet concentration is 800 ppm. For the other operation modes to be able to produce this quantity of CO<sub>2</sub>, or for this to happen no matter the inlet concentration, more stages would be necessary. The design goal requires, therefore, some adjustments. As it is, an adsorber with 10 stages, each stage with 10 cm bed height, operating at a superficial velocity of 0.23 m/s and a sorbent flow rate of 60 kg/h, has a residence time of sorbent of 34 minutes. The sorbent loading exiting the adsorber is determined based on 2 assumptions: the first one is that the sorbent entering the adsorber already has a loading of 0.21 mol/kg, the equilibrium loading at 400 ppm and 70°C (desorption conditions); the second assumption is that the sorbent loading after a certain residence time in the adsorber is equivalent to the loading after that same time in a closed system - the loading at residence time (RT) is the same as the loading at  $t=RT$  from the breakthrough curve.

As has been mentioned in section 5, at a higher flow

rate and superficial velocity of air, the uptake of CO<sub>2</sub> on the sorbent is faster. However, as the loading increases, the efficiency of the adsorption under high superficial velocities decreases compared to that of lower superficial velocities. So, as it is advantageous to have a high flow rate of air when the sorbent has a low loading, and smaller flow rate when it increases, a simple solution presents itself. Instead of the flow rate of incoming air being equally distributed through the 10 stages of the adsorber, it can be unequally distributed, with the higher flow rate to the top stages and a lower one to the bottom stages. So, in this sense, the flow rate was distributed through the 10 stages as shown in Table II.

**TABLE II:** Description of the stages in the adsorber, with superficial velocity, corresponding flow rate, residence time and pressure drop across the bed. Stages are numbered from top to bottom.

stages	$u_0$	flow rate	residence time	$\Delta P$
#	(m/s)	(m <sup>3</sup> /h)	(min)	(Pa)
1-4	0.305	138	2.4	185.2
5-8	0.220	99.5	3.5	276.7
9-10	0.120	54.3	4.9	384.3
<b>TOTAL</b>	-	1059	33.5	2616

### 6.3. Desorption column dimensions

Based on these assumptions, the sorbent will leave the adsorber with a loading of 0.39 to 0.62 mol/kg, depending on the inlet concentration. The desorber works as a PFR in counter-current, with sorbent flowing from stage to stage through the downcomers, and the air flowing up through all stages, at 70°C. The stages are heated by flowing hot water around the walls of the desorber and by heating the plates where the beds rest upon. As the fluidization mixes the sorbent within the bed and promotes heat transfer by forced convection, it can be assumed that the temperature is homogeneously distributed through the bed.

Qian Yu, *et. al.*<sup>10</sup> studied the desorption of sorbent after direct air capture in one tall fluidized bed using air as purge, at temperatures between 67 and 72 °C, at different residence times. They concluded that the desorption is more kinetic than equilibrium controlled, but did succeed in producing a continuous stream of 1% v/v CO<sub>2</sub>-enriched air.

The assumption that in 23 minutes of residence time, at 70°C with air as purge at a flow rate of 55 m<sup>3</sup>/h, the sorbent loading is reduced from between 0.39 and 0.62 mol/kg to 0.21 mol/kg cannot be validated at this point. However, the results of Qian Yu, *et. al.*, support this assumption, as the production of a continuous product gas with 1% CO<sub>2</sub> with a residence time of 34 minutes and a similar superficial velocity.

The design for the desorber is a 5-stage fluidized bed with 40 cm diameter, operating at 0.14 m/s of air superficial velocity. However, it is not advantageous to have all stages with the same height and thus, with equal sorbent residence time. This is mainly because, on the top stage, the purge air already has a significant concentration of CO<sub>2</sub> and, as the loading of the sorbent is not so high to start with, the loading on



the sorbent is close to the equilibrium loading at that set of temperature and  $\text{CO}_2$  concentration. On this stage, there may even occur adsorption, to some degree. However, as the loading of the sorbent is close to the equilibrium loading at said conditions, the adsorption rate is so low that it will not be significant given a short contact time of solid and gas phases. At the same time, the driving force for desorption is low and no significant  $\text{CO}_2$  is released from the sorbent to the air on this stage. Given these aspects, the residence time in the top stage should be short, and this stage's purpose is that of increasing the temperature of the sorbent to desorption temperature. To reduce the residence time, without changing the sorbent flux, the bed height must be decreased which, in turn, increases the heat transfer efficiency because it decreases the volume to heat transfer area ratio. With a bed height of 3 cm, the residence time is about 1.4 minutes, which theoretically is enough time for the sorbent's temperature to increase to  $70^\circ\text{C}$ .

For similar reasons, the second stage from the top should also have a shorter residence time than the one below, which should have a shorter residence time than the next one, and so forth. This way, the bed height increases from top stage to bottom stage. Because the sorbent and air contact in cross-flow, on the bottom stage the air is leanest and the sorbent is heated at  $70^\circ\text{C}$ , therefore heat transfer is not a limitation on this stage and the bed can be tall, at 15 cm. This allows more contact time of the sorbent with the air, therefore, more efficient desorption until equilibrium. On this stage, the sorbent is, however, already close to being lean so, on the second to bottom stage the air does not have a very high concentration of  $\text{CO}_2$ , therefore can still desorb efficiently. Thus, this stage can also have a high residence time, meaning, a taller bed of 15 cm. On the third and middle stage the  $\text{CO}_2$  concentration is already higher, so a more shallow bed, of 10 cm, is more reasonable, to decrease the contact time and allow the desorption to favour above the adsorption. On the second to top stage, this is even more pressing, therefore, the contact time should be even shorter, decreasing the bed height to 7 cm. This way, the total residence time of the sorbent in the desorber remains the same, 23 minutes, but it is unevenly distributed through the stages, increasing from top to bottom.

It is important to note that, even though the concentration of  $\text{CO}_2$  in the air stream can be estimated in relative terms, the precise concentration or the variation of the desorption efficiency with contact time are not known, because the desorption in these conditions could not be studied with the available setup.

The table below, III, shows the bed heights, residence times and pressure drop (calculated with equation 5) of each stage, as well as the total.

The final design for the setup can be seen in Figure 12.

## 7. Energy cost analysis

In order to estimate the overall energy costs of operating the setup, the calculations described by equations 8 to 11 can be applied to the final design. It is impor-

**TABLE III:** Description of the 5 stages in the desorber, with bed height, corresponding residence time and pressure drop across the bed. Stages are numbered from top to bottom.

stage #	bed height (cm)	residence time (min)	pressure drop (Pa)
1	3	1.4	108.2
2	7	3.2	252.6
3	10	4.6	360.8
4	15	6.9	541.2
5	15	6.9	541.2
<b>TOTAL</b>	<b>50</b>	<b>23.1</b>	<b>1804.1</b>

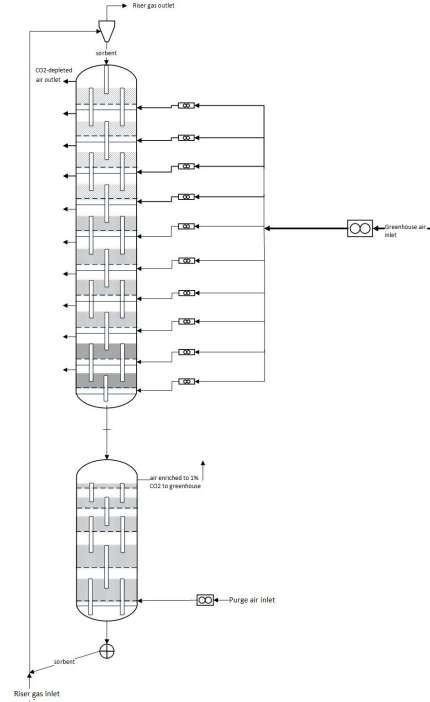


**FIG. 12:** Inside view of the final design of the setup.

tant to note that the energy costs are obtained in units of kJ per kg of desorbed  $\text{CO}_2$  which, given the efficiency of the desorption process, corresponds to 1.7 kg  $\text{CO}_2$  actually adsorbed on the sorbent, which is relevant for the calculation of the heat to be provided in the desorber to increase the temperature to  $70^\circ\text{C}$ . Another important note is that, despite the goal of producing 1 kg/h of  $\text{CO}_2$ , the average and pessimistic value of 1 kg of  $\text{CO}_2$  per 1.3 hours was used.

The energy demand values of the different factors in the operation of this setup are seen in Figure 13. It is clear that the biggest energy penalty is, by far, the energy spent on compressing the air that goes into the adsorber, making up almost three quarters of the total energy costs. This is due to the fact that every one of the 10 stages has a separate inlet flow of air, unlike the desorber. In the desorber, not only is the total flow rate of air a lot smaller than in the adsorber, but the pressure drop along all stages is cumulative. This is not the case in the adsorber, where in every stage the weight of the bed has to be overcome by a different stream, and a different fan.

By comparison, the contribution of the compression of air for the desorber and riser and the heat necessary for the heating of the  $\text{CO}_2$  are negligible. Therefore, in terms of economic analysis of operating this setup,

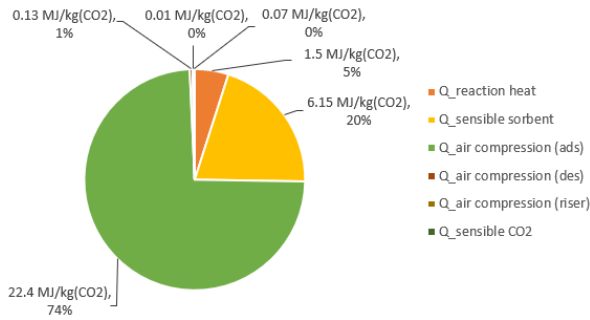


FIG. 13: Energy demands of the different operations of the setup.

the most relevant parameters are the contacting energy and costs in the adsorption, in terms of electric costs, and the heating in the desorption, in terms of thermal energy.

The contacting energy, as described by Qian Yu<sup>20</sup>, is calculated by the following equation 12, where  $\Delta P$  is the pressure drop along the bed and  $\eta_g$  is the gas efficiency of adsorption, determined by equation 13.

$$E(J/g) = \frac{\Delta P(Pa)}{\eta_g \cdot C_{CO_2}(g/m^3_{air})} \quad (12)$$

$$\eta_g = \frac{C_{CO_2} \cdot t - \int_0^t C_{CO_2} dt}{C_{CO_2} \cdot t} \quad (13)$$

Because in each adsorption stage new air is contacted with the sorbent, the gas efficiency has to be calculated for each stage and not as a whole unit. For calculation purposes, the average inlet concentration of 600 ppm was used, as well as the breakthrough curve at this concentration, to determine the integral.

The sum of the contacting energy of all adsorption stages is approximately 3.5 kJ/g<sub>CO<sub>2</sub></sub>. With the cost of electricity, the contacting cost can be determined, using the conversion described in equation 14. The cost of electricity, for businesses in the Netherlands, is estimated at 0.16 €/kWh<sup>21</sup>.

$$C_{cont} = \frac{E}{3.6 \times 10^6} \cdot C_{elect} \quad (14)$$

Given this, the contacting cost of the adsorption process is 0.15 €/kg<sub>CO<sub>2</sub></sub>.

As for the cost of regeneration of the sorbent, these are mostly composed of the cost of the thermal energy required to heat up the sorbent and to overcome the endothermicity of the desorption reaction. Qian Yu<sup>20</sup> simplified this calculation as described in equation 15.

$$C_{reg} = \left( \Delta H_r + \frac{C_{p,sorb} \cdot (T_{des} - T_{ads})}{(q_e - q_{des}) \cdot \eta_s \cdot MW_{CO_2}} \right) \cdot C_{therm} \quad (15)$$

$$\eta_s = \frac{q_t - q_{des}}{q^* - q_{des}} \quad (16)$$

$\Delta H_r$  is the heat of reaction, at 65 kJ/mol<sup>18</sup>,  $\eta_s$  is the solid efficiency, calculated with equation 16, where  $q_t$  is the sorbent loading at the end of the adsorption process, here using the average value of 0.47 mol/kg, and the thermal energy cost, from natural gas for businesses in the Netherlands is estimated at 3.44 €/GJ<sup>22</sup>. The final cost of the desorption is, thus, 0.03 €/kg<sub>CO<sub>2</sub></sub>.

Considering that the goal of producing 1 kg of CO<sub>2</sub> an hour is achieved, with higher concentrations of CO<sub>2</sub>

in the air and non-degraded sorbent, the cost of operating the setup is set at 0.18 €/h, or 180 €/ton<sub>CO<sub>2</sub></sub>.

The cost of industrial CO<sub>2</sub> is between 80 and 180 €/ton. This means that running the air capture setup has the same cost than the more expensive supply of industrial CO<sub>2</sub>. However, in a future where CO<sub>2</sub> emissions get taxed, it may end up being cheaper or to apply such an installation in industrial greenhouses. Besides, just like many of the sustainable measures, the cost does not justify emissions of pollutants, given their environmental impact.

## 7.1. Conclusion and Recommendations

Regarding the final design and the process followed to reach it, a few important notes need to be discussed. It's important for the reader to retain that this is a preliminary design, obtained from preliminary data and calculations.

Firstly, the breakthrough curves, on which the values of sorbent loading and amount of CO<sub>2</sub> adsorbed were based on, were obtained with somewhat degraded sorbent. This indicates that, using fresh non-degraded sorbent in the installation, the sorbent loading leaving the adsorber is higher than the one determined and, therefore, more CO<sub>2</sub> can be desorbed and a higher concentration on the product stream can be achieved. However, even though the equilibrium loading under these conditions with fresh sorbent can be estimated using the Toth isotherm and its parameters, determined by M. Bos<sup>12</sup>, the uptake rate and shape of the resulting breakthrough curve cannot be accurately predicted. This way, the calculations of sorbent loadings and production of CO<sub>2</sub> enriched stream in the designed setup should be seen as those of a pessimistic scenario, when the sorbent approaches the end of its lifetime, with the confidence that it is more efficient through most of the operation of this installation.

Given this, the calculated costs are higher than the resulting costs of using non-degraded sorbent. This because the operation costs remain the same, but the amount of CO<sub>2</sub> obtained is higher. These costs are determined based only on operation, excluding investment costs and maintenance. For a fully detailed economic analysis, more extensive data and calculations would need to be performed, mainly data on adsorption in this setting of cross-flow, validating the approximation of using residence time in a stage as absolute time in the closed stage where the breakthrough curve was obtained, and more extensive data on the desorption under the selected conditions.

Besides this, the data obtained and the calculations made were for dry air, neglecting the humidity in the air in the greenhouse. This is a very important factor, because it is known that the presence of water increases the CO<sub>2</sub> capture capacity of the sorbent, but also increases the heating requirements of the desorption process. Therefore, for further development of this setup, also this aspect requires further study.

## Bibliography

<sup>1</sup>Rajesh A Khatri, Steven Chuang, Yee Soong, and McMahan Gray. Thermal and chemical stability of regenerable solid amine sorbent for co 2 capture. *Energy & Fuels - ENERG FUEL*, 20, 07 2006.

- <sup>2</sup>Abass A. Olajire. Co2 capture and separation technologies for end-of-pipe applications – a review. *Energy*, 35(6):2610 – 2628, 2010. 7th International Conference on Sustainable Energy Technologies.
- <sup>3</sup>Klaus S. Lackner, Sarah Brennan, Jürg M. Matter, A.-H. Alissa Park, Allen Wright, and Bob van der Zwaan. The urgency of the development of co2 capture from ambient air. *Proceedings of the National Academy of Sciences*, 109(33):13156–13162, 2012.
- <sup>4</sup>Bryce Dutcher, Maohong Fan, and Armistead G. Russell. Amine-based co2 capture technology development from the beginning of 2013—a review. *ACS Applied Materials & Interfaces*, 7(4):2137–2148, 2015. PMID: 25607244.
- <sup>5</sup>M.C. Sánchez-Guerrero, P. Lorenzo, Evangelina Medrano, N. Castilla, María Soriano, and A. Baille. Effect of variable co2 enrichment on greenhouse production in mild winter climates. *Agricultural and Forest Meteorology*, 132:244–252, 10 2005.
- <sup>6</sup>Elif Erdal Ünveren, Bahar Özmen Monkul, Serife Sarioğlu, Nesrin Karademir, and Erdogan Alper. Solid amine sorbents for co2 capture by chemical adsorption: A review. *Petroleum*, 3, 12 2016.
- <sup>7</sup>Rens Veneman, Natalia Frigka, Wenying Zhao, Zhenshan Li, Sascha Kersten, and Wim Brilman. Adsorption of h2o and co2 on supported amine sorbents. *International Journal of Greenhouse Gas Control*, 41:268 – 275, 2015.
- <sup>8</sup>Adam Berger and Abhoyjit Bhowm. Optimizing solid sorbents for co2 capture. *Energy Procedia*, 37:25–32, 12 2013.
- <sup>9</sup>Klaus S. Lackner. The thermodynamics of direct air capture of carbon dioxide. *Energy*, 50:38–46, 02 2013.
- <sup>10</sup>Qian Yu. *Direct Capture of CO2 from Ambient Air using Solid Sorbents*. PhD thesis, University of Twente, Netherlands, 10 2018.
- <sup>11</sup>R. Veneman. *Adsorptive systems for post-combustion CO2 capture*. PhD thesis, 09 2015.
- <sup>12</sup>Martin Bos. *Storage of renewable electricity in methanol: Technology development for CO2 air capture and conversion to methanol*. PhD thesis, 06 2019.
- <sup>13</sup>Duong D. Do. *Adsorption Analysis: Equilibria and Kinetics*. Published by Imperial College Press and distributed by World Scientific Publishing Co., 1998.
- <sup>14</sup>F. G. Helfferich. Principles of adsorption & adsorption processes, by d. m. ruthven, john wiley & sons, 1984, xxiv + 433 pp. *AIChE Journal*, 31(3):523–524, 1985.
- <sup>15</sup>Reactor types and catalysts test. Accessed: 2019-04-08.
- <sup>16</sup>Daizo Kunii and Octave Levenspiel. Chapter 3 - fluidization and mapping of regimes. In Daizo Kunii and Octave Levenspiel, editors, *Fluidization Engineering (Second Edition)*, pages 61 – 94. Butterworth-Heinemann, Boston, second edition edition, 1991.
- <sup>17</sup>Rick T. Driessen. Development of a multistage fluidized bed for deep h2s removal from natural gas. Master's thesis, University of Twente, 2016.
- <sup>18</sup>Martin J. Bos, Vincent Kroeze, Stevia Sutanto, and Derk W. F. Brilman. Evaluating regeneration options of solid amine sorbent for co2 removal. *Industrial & Engineering Chemistry Research*, 57(32):11141–11153, 2018.
- <sup>19</sup>Rick T. Driessen, Martin J. Bos, and Derk W. F. Brilman. A multistage fluidized bed for the deep removal of sour gases: Proof of concept and tray efficiencies. *Industrial & Engineering Chemistry Research*, 57(11):3866–3875, 2018.
- <sup>20</sup>Q. Yu and D.W.F. Brilman. Design strategy for co2 adsorption from ambient air using a supported amine based sorbent in a fixed bed reactor. *Energy Procedia*, 114:6102 – 6114, 2017. 13th International Conference on Greenhouse Gas Control Technologies, GHGT-13, 14-18 November 2016, Lausanne, Switzerland.
- <sup>21</sup>euostat - statistics explained, statistieken over elektriciteitsprijzen. [https://ec.europa.eu/eurostat/statistics-explained/index.php?title=Electricity\\_price\\_statistics/nl](https://ec.europa.eu/eurostat/statistics-explained/index.php?title=Electricity_price_statistics/nl). Accessed: 2019-09-30.
- <sup>22</sup>infogram - hoeveel kost 1 kwh elektriciteit/aardgas? <https://infogram.com/hoeveel-kost-1-kwh-elektriciteit/aardgas/-prijzen-voor-kleine-professionele-afnemers-all-in-exl/-btw-1hnq41nlj1/1p63z>. Accessed: 2019-09-09.